Hemerythrin: Alternative Oxygen Carrier

Nature has developed an effective transport protein with a binuclear iron center in place of a heme.

Irving M. Klotz, Gerald L. Klippenstein, Wayne A. Hendrickson

In the course of biological evolution, nature has developed several alternative molecular devices to provide for oxygen transport in tissues. Hemoglobin is the most frequently occurring of these since it appears in all vertebrates and in many invertebrate species. Among the latter, however, the oxygen-carrying pigments are often the nonheme proteins, hemerythrin and hemocyanin. Despite their functional resemblances, there are great differences among the three oxygen carriers with respect to their macromolecular structure and the molecular nature of the oxygen-holding site.

A comparison of some of the characteristics of these oxygen carriers is provided in Table 1. Two of the proteins, hemoglobin and hemerythrin, have Fe at the active site; the third, hemocyanin, has Cu. Although the prefix heme implies to chemists and biologists the presence of an iron-porphyrin ring, that was not the original intent (*1*) when the word "heme" was adopted from the Greek word for blood. Hemerythrin and hemocyanin contain no porphyrin. Nevertheless, all three blood proteins are strikingly colored in their oxygenated states, hemoglobin its familiar red, hemerythrin an unusual violet with reddish tint, and hemocyanin a blue reminiscent of cupric salts but much more intense. In the deoxygenated state, the absence of the porphyrin manifests itself in the complete loss of visible absorption bands, that is, of color, in hemerythrin and in hemocyanin. Also at the simplest chemical level, stoichiometry of oxygen uptake, there are fundamental differences: in hemoglobin this stoichiometry is 1Fe : O_2, in hemerythrin it is 2Fe : O_2, in hemocyanin it is 2Cu : O_2. There are, in addition, major differences in molecular weight, number, and arrangement of subunits in the quaternary structure and amino acid composition and sequence.

Nevertheless, hemerythrin, hemocyanin, and hemoglobin, in spite of all their differences, function effectively as oxygen carriers. It is intriguing to establish the extent to which different molecular components and structures have been adapted by alternative evolutionary pathways in nature to perform the same physiological function, in this case, transport of oxygen. For such studies, hemerythrin has proved to be a much more tractable material than hemocyanin in that it can be isolated in a clearly defined homogeneous state and can be readily crystallized. Thus, enormous strides have been made in elucidating its structure at all levels of atomic and molecular resolution. This article is devoted to a description of structure and function in hemerythrin.

Size, Symmetry, and Subunit Constitution

Hemerythrin has been found in animals of four different invertebrate phyla: sipunculans, polychaetes, priapulids, and brachiopods. Within an organism, hemerythrin is found primarily in the coelom. A different hemerythrin occurs in the vascular system and still another, myohemerythrin, is found in muscle. As with hemoglobins, there are molecular differences between hemerythrins of different origin but, nevertheless, common structural patterns. A lowly sipunculan worm, *Phascolopsis* (syn. *Golfingia*) *gouldii*, a native of the North American Atlantic coast, has provided material for most of the original molecular investigations, and hence we have used hemerythrin as the "standard" for interrelating structure and function.

Hemerythrin, like hemoglobin, is carried in erythrocytes. The pigment isolated from these cells exists as an octamer (Table 2) with a molecular weight near 100,000 (*2–7*), except in *Phascolosoma agassizii* (*6*) where it occurs, surprisingly, as a trimer, a relatively rare quaternary arrangement (*8, 9*). A myohemerythrin isolated from the retractor muscle of *Themiste pyroides* (*4*) exists as a monomer, as does myoglobin in the heme series of oxygen carriers.

The molecular dimensions of hemerythrin and its subunits are now known from the x-ray diffraction results described below. Myohemerythrin, and similarly the subunits of octameric hemerythrin, can be circumscribed by an ellipsoid with axes of 30 by 44 by 28 Å (*10*). Octameric hemerythrin has approximate external dimensions of 75 by 75 by 50 Å (*11*).

All octameric hemerythrins can be dissociated into monomeric species. The relationships between monomer and octamers of different oxidation states of hemerythrin are illustrated in Fig. 1. Oxidation state per se does not play a role in maintenance of the octameric ensemble. The cysteine sulfhydryl group, however, is crucially involved, for its modification leads stoichiometrically to conversion of octamers to monomers (*12*). Exposure to gross denaturants, such as sodium dodecyl sulfate (*2*), or placement of multiple charges on the macromolecule, for example by succinylation (*13*), also dissociates the octamer into monomers.

A priori a large number of possible geometric arrangements could be constructed for an octamer. However there are reasonable restrictions that can be imposed on them. Since the monomers of a given hemerythrin are generally essentially identical, each subunit of the octamer may be assumed to be in an equivalent or quasi-equivalent environment. Thus, the array of subunits is expected to form a closed set associated about a central point, that is, must have a particular point group symmetry. A further restriction derives from the optical asymmetry of proteins, which precludes symmetry operations of inversion. Only two symmetries are available to an octamer comprising identical, handed objects. One is the cyclic point group C_8 with subunits arranged in head-to-tail fashion about an eightfold axis. The other is the dihedral point group D_4 (422 in the "International" notation) with sub-

Dr. Klotz is Morrison Professor at Northwestern University, Evanston, Illinois 60201. Dr. Klippenstein is Associate Professor of Biochemistry, University of New Hampshire, Durham 03824. Dr. Hendrickson is a member of the Laboratory for the Structure of Matter, Naval Research Laboratory, Washington, D.C. 20375.

units related by a fourfold axis and four perpendicular twofold axes of two kinds.

In general each unit in a D_4 octamer can interact with every other unit through one of six types of contact. However for globular units, such as are found in proteins, only three types of interactions are likely: those between adjacent units related by the fourfold axis and those between nearest neighbors related by either of two kinds of twofold axes. The integrity of the octamer requires that bonding associations be maintained either at the fourfold axis and at least one kind of twofold contact or alternatively at both kinds of twofold contacts though not necessarily at the fourfold contacts (*14*). Thus there are three classes of probable packing for a D_4 protein composed of globular subunits: that with fourfold and both kinds of twofold contacts, that with fourfold and only one kind of twofold contact, and that with only both kinds of twofold contacts. These have 16, 12, and 8 bonding interfaces, respectively. An octamer with C_8 symmetry would also have eight bonding regions. An instructive example of D_4 symmetry is given by the regular, closest packing of eight spheres. This has two possibilities, arrangements at the vertices of a square antiprism or at the vertices of a cube (a special square prism). These correspond to the first two of the general classes. For irregular subunits the distinction between the different classes blurs since the extent of interaction can vary at different types of interfaces. But other things being equal, one would expect the array with the largest number of contact interfaces to be the most stable. Thus for hemerythrin, the first D_4 class, analogous to the square antiprism, is the most probable geometric arrangement of subunits (*8*).

The first hard evidence on hemerythrin symmetry came from a study on a crystal form of *Phascolopsis gouldii* hemerythrin which showed exact fourfold symmetry and strong noncrystallographic symmetry indicating a close approximation to D_4 molecular symmetry (*15*). Qualitative features of the diffraction pattern from these crystals indicated that the molecule is more like a square prism than a square antiprism. More recently, crystals of *P. gouldii* hemerythrin B have been grown that crystallographically express the full D_4 molecular symmetry (*11*). The low-resolution x-ray structures of *P. gouldii* and *T. dyscritum* hemerythrins (described below) show the subunit arrangement to be intermediate between the geometries analogous to a cube and a square antiprism. Contacts are made across both kinds of twofold axes, but those of one kind of twofold are predominant (*11, 16*).

Table 1. Some properties of protein oxygen carriers.

Item	Hemoglobin	Hemerythrin	Hemocyanin
Metal	Fe	Fe	Cu
Oxidation state of metal in deoxy protein	(II)	(II)	(I)
Metal : O_2	Fe : O_2	2Fe : O_2	2Cu : O_2
Color, oxygenated	Red	Violet-pink	Blue
Color, deoxygenated	Red-purple	Colorless	Colorless
Coordination of Fe	Porphyrin ring	Protein side chains	Protein side chains
Molecular weight	65,000	108,000	400,000 to 20,000,000
Number of subunits	4*	8†	Many

*In some species (for example, *Glycera*) hemoglobins are monomeric, in others (for example, *Arenicola*) they are multisubunit oligomers with molecular weights in the millions. †See also Table 2.

Table 2. Comparison of subunit constitution in hemerythrin.

Species	Molecular weight	Number of monomers
Phascolopsis (syn. Golfingia) gouldii	108,000	8
Sipunculus nudus	100,000	8
Themiste (syn. Dendrostomum) pyroides		
Erythrocyte	100,000	8
Muscle	13,900	1
Themiste (Dendrostomum) dyscritum	103,000	8
Phascolosoma agassizii	40,600	3
Lingula unguis	110,000	8

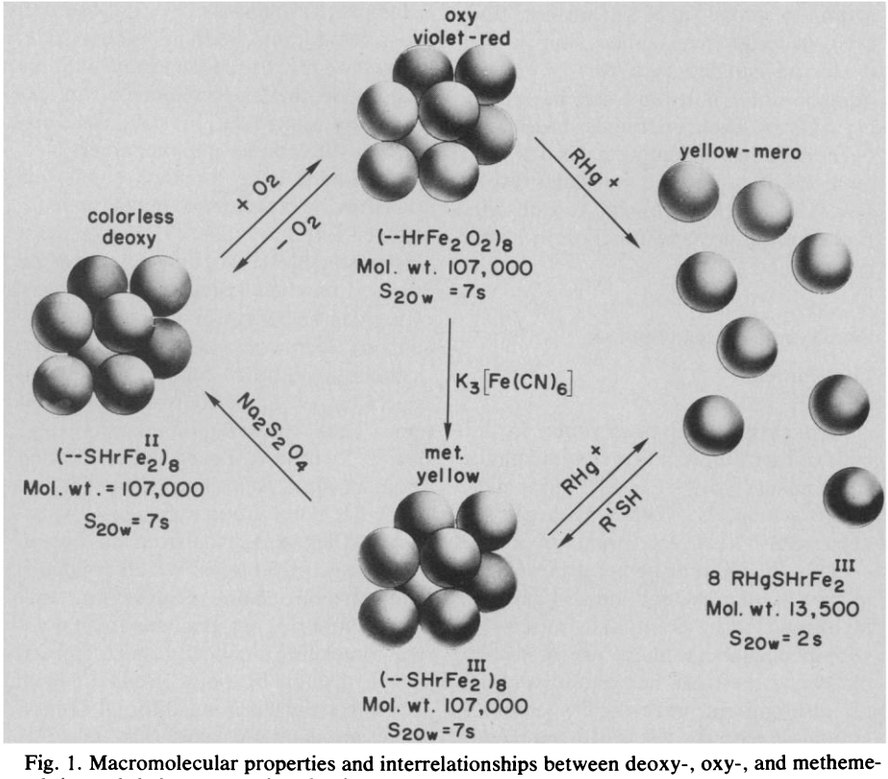

Fig. 1. Macromolecular properties and interrelationships between deoxy-, oxy-, and methemerythrin, and their monomeric subunit.

Molecular Structure of the Protein

Primary structure. Complete amino acid sequences have been established for hemerythrin of *P. gouldii* (*17*) and myohemerythrin from *T. pyroides* (*18*). Information is also available for erythrocyte

hemerythrin from *T. pyroides* (*19*), for some of the variants found in *P. gouldii* (*20*) and for segments near the termini of one of the *Phascolosoma agassizii* hemerythrins (*21*).

The primary structure of *P. gouldii* hemerythrin is illustrated in Fig. 2. Four Pro residues (*22*) are immediately seen among the first dozen at the NH_2-terminal end of the polypeptide. In view of the sharp bend often associated with a Pro residue, one would expect a nonhelical conformation for this NH_2-terminal section. Another particularly interesting feature is the presence of a single Cys residue (at position 50) near the center of the polypeptide chain. It is the blocking of this SH group that leads to dissociation of the octamer. Interestingly, trimeric (*6*), and monomeric (*18*) hemerythrins do not have an SH group at residue 50. Distributed throughout the chain are other possible ligands holding the Fe atoms, namely Lys, Tyr, His, Met, Asp, and Glu residues, which are present in particularly high concentrations between positions 18 to 26, 67 to 78, and 101 to 112.

Sequence data have been accumulated also for hemerythrins from other species, for genetic variants, and for myohemerythrin. This information has been very useful for, among other things, reducing the number of possible ligands to the active center iron atoms, and in interpreting x-ray diffraction patterns. This information also serves to identify especially significant structural elements. For example, although the sequences of *P. gouldii* hemerythrin and *T. pyroides* myohemerythrin are only 45 percent homologous overall, the homology is much higher than average at the COOH-terminus (79 percent for residues 95 to 113) and at the NH_2-terminus (62 percent for residues 1 to 26).

Multiple hemerythrin variants in erythrocytes of a single species are often encountered. Five variants in *P. gouldii* have been identified (*20*) which fall into two major classes, designated A and B. Hemerythrin A consists of four variants arising from interchanges of Thr and Gly at position 79 and of Ser and Ala at position 96. Hemerythrin B is a single component, which is different from any of the A variants in having a Glu at residue 63, Asp at 78, and Asn at 92 replacing Gln, Glu, and His, respectively, and only Gly and Ala at the respective positions 79 and 96.

Variants have also been found in *Phascolosoma agassizii* where three major subunit types occur (*6*), in *Lingula* (*5*) where two major hemerythrins have been found, in *Priapulus caudatus* (*23*) and in *T. pyroides* (*20*). An organism such as *T. dyscritum* (*7*), in which hemerythrin apparently occurs as a single component, is exceptional.

Secondary structure. Some insight into secondary structure is provided by the circular dichroic spectra of hemerythrin. Rotatory behavior in the ultraviolet range arises primarily from the peptide bonds and from amino acid side chains of the protein itself. In the vicinity of the $n \rightarrow \pi^*$ and $\pi \rightarrow \pi^*$ peptide absorptions, strong negative ellipticities are found at 222 and 209 nm for methemerythrin, and a positive band appears at 197 nm (*4, 24*). Helical polypeptides show bands at 222, 206 to 207, and 190 to 192 nm (*25*). If this spectrum is attributed entirely to helix then the magnitude of the ellipticities suggests that hemerythrin is about 75 percent helical and has little or no β-structure.

Information about polypeptide conformation is also implicit in the primary structure. Various empirical procedures have been developed to predict the location of elements of secondary structure (α-helix, β-sheet, β-turns, and random coil) from the amino acid sequence. The rules of Chou and Fasman (*26*) predict a helix content of 50 to 55 percent and a β-sheet content of 16 percent for the hemerythrin molecule (*27*). These rules also predict the specific locations of these elements and of turns between them. For example, one would expect one or two β-turns in the NH_2-terminal section.

Solid evidence about the secondary structure of hemerythrin can be deduced from the x-ray work. Measurements of the lengths of helix rods in the low-resolution density maps indicate that 70

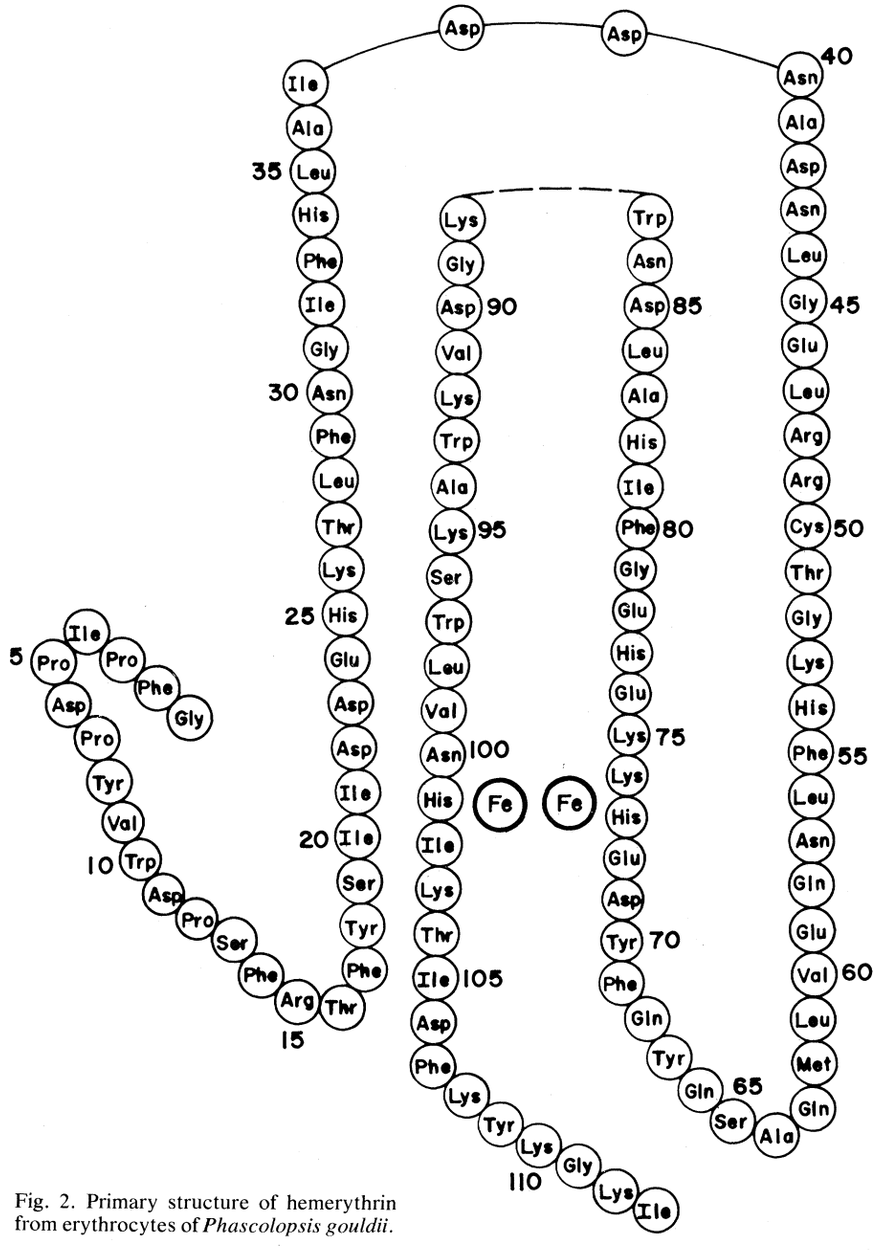

Fig. 2. Primary structure of hemerythrin from erythrocytes of *Phascolopsis gouldii*.

to 75 percent of the residues are in helices (*10, 16*), which agrees well with the circular dichroism results. The x-ray results also corroborate the location of four of the six turns predicted from the sequence, including two crucial turns at corners between helices. There is no evidence of β-sheet structure.

Tertiary structure. The three-dimensional folding of the polypeptide chains within hemerythrin subunits is now known from x-ray crystallographic analyses. That hemerythrins can readily be crystallized has long been known (*28, 29*), but crystals suitable for structure analysis had evaded discovery until recently. Suddenly new crystals have led to structure determinations for three hemerythrins: the monomeric myohemerythrin from *T. pyroides* (*10*) and coelomic octamers from *P. gouldii* (*11*) and *T. dyscritum* (*16*). These studies are still at low resolution but extensions to higher resolution are progressing.

An exceptional amount of structural information has been derived from the 5.5-Å resolution electron density map of myohemerythrin in the first of these studies. The quality of the map, high helix content of the molecule, and recourse to the abundant chemical data on hemerythrin facilitated a rather detailed description of the course of the polypeptide chain in relation to the dimeric iron center. This image of myohemerythrin was also used to solve the structure of *P. gouldii* hemerythrin B by molecular search techniques. An independent analysis of *T. dyscritum* hemerythrin has been completed to 5-Å resolution by the single isomorphous replacement method. Although the resulting map was not as accurate as that for myohemerythrin, the four independent views of the subunits in this crystal helped to compensate and enables one to trace the main chain in a course very similar to that found for myohemerythrin.

All three molecules have a common tertiary structure—the hemerythrin fold. The picture of the hemerythrin subunit which emerges from the x-ray work is illustrated by the tubing model drawn in Fig. 3 and by the individual monomers shown in Fig. 4. The most salient features of this structure are four interconnected, quasi-parallel helix segments and the active iron center which they embrace. A rather tortuous arm of more-or-less extended polypeptide chain is appended to one end of the helix core, and a short stub of compact, probably helical chain closes off the other end. By reference to sites of heavy atom binding and positions of histidine residues implicated as iron ligands, the amino acid sequence

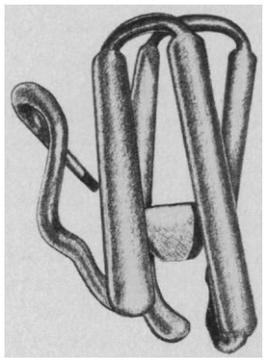

Fig. 3. Molecular model of hemerythrin monomer at low resolution. Tubes represent helical segments. [Courtesy of the *Proceedings of the National Academy of Sciences*]

could be aligned with these structural features in myohemerythrin. On the basis of this alignment a nomenclature was adopted to identify the extended segment at one end as the NH_2-terminal arm; the four major helices successively as A, B, C, and D; the corners between helices as AB, BC, and CD; and the COOH-terminal segment as the E helical stub. This description applies to all three molecules. The only structural difference evident at low resolution is the abbreviation of the CD corner in octamer subunits due to the deletion of five residues as compared to the myohemerythrin sequence.

Recently, the above interpretation has been extended and quantified by building an atomic model of the polypeptide backbone. The model was constructed to fit the electron density distribution for myohemerythrin while meeting several conditions for stereochemical reasonableness (*30*). An adaptation of this model served also to explain the electron density map for *P. gouldii* hemerythrin. The α-carbon skeleton of the *P. gouldii* model is shown in Fig. 5. According to this model, the residues included in helical segments are 18 to 38 for helix A, 40 to 62 for B, 69 to 84 for C, 88 to 105 for D, and 107 to 113 in a quite distorted helix for E.

A particularly interesting and simplifying aspect of hemerythrin structure is the presence of an approximate diad axis relating one third of a subunit to another third. This axis runs roughly parallel to the major helices and passes through the iron center. Evidence of the pseudo symmetry is given by a correlation coefficient of 0.52 between the electron density distribution of the A-B helix pair and that of the C-D pair after twofold rotation. The primary structures reflect this apparent pseudosymmetry as well in that an apparent sequence repeat occurs within the polypeptide chain. In myohemerythrin, for example, the segment consisting of residues 25 to 67 is 32 percent homologous with 73 to 114 if one allows a four-residue gap after residue 42 and a five-residue gap after residue 90 (*18*). Analogous segments can be seen in erythrocyte hemerythrins, albeit with slightly lower homology.

Quaternary structure. The mode of subunit arrangement in octameric hemerythrin is essentially identical in the *P. gouldii* and *T. dyscritum* structures and is as illustrated in Fig. 4. The subunits are each in an identical or quasi-identical environment by virtue of the D_4 symmetry. The long (pseudodiad) axes of the subunits lie roughly perpendicular to the fourfold axis (R). The molecule is composed of two layers, each a square of four subunits related by R in an end-to-side arrangement. The layers are related to one another by four twofold axes of two kinds (P and Q). This formation leaves a square channel along R, each side being 20 Å long. The channel swells to a central chamber 30 Å in diameter and 15 Å high. The molecule as a whole resembles a square doughnut.

The subunits of hemerythrin interact by way of three types of subunit interfaces. Within layers, the BC corner and E stub at the end of one subunit are in contact with parts of the B and C helices at the side of a neighboring subunit. The association between subunits 1 and 2 in Fig. 4 typifies the eight such R interfaces in the molecule. The major interaction between subunits of different layers is that between neighbors related by Q axes (such as 1 and 8 or 4 and 5 in Fig. 4). Parts of the NH_2-terminal arm and A and B helices of adjacent subunits interact isologously at these interfaces. Less extensive contacts are made across the P axes which relate the COOH-terminus of the E stub and the juncture between the NH_2-terminal arm and helix A of one subunit with the same area of another (see pairs 2 and 6 and 4 and 8 in Fig. 4). There are four each of the P and Q interfaces. Residues with potential for intersubunit contact have been identified by noting the pairs of α-carbon atoms from different subunits which are within 10 Å of each other in the tentative atomic model for the polypeptide backbone of *P. gouldii* hemerythrin (*30*). This analysis suggests that the relative importance of individual P, Q, and R interfaces in stabilizing the octamer is in the contact ratio 22 : 71 : 41. An examination of the *T. dyscritum* electron density map gives a similar impression: there are weak density connections at R interfaces, major connections between layers at Q interfaces, but no connection between layers at P interfaces.

Active Site

The Fe to O_2 stoichiometry (*29, 31, 32*) of 2 : 1 in itself suggests that the two Fe atoms are close to each other, with the O_2 molecule perhaps forming a bridge between them. Extensive spectroscopic and magnetic studies have established unequivocally the juxtaposition of two antiferromagnetically coupled Fe atoms and their electronic structure. The electronic structure of the bound O_2 has also been clearly delineated, but the precise location of O_2 with respect to each Fe atom is still ambiguous.

The x-ray diffraction results give a precise Fe. . .Fe distance (3.44 Å) and, coupled with chemical studies and sequence data, point strongly to specific residues as the ligands holding the iron atoms to the protein matrix. The tentative picture of the active site that emerges is illustrated in Fig. 6.

Spectroscopy. Spectroscopic and magnetic studies have focused on a comparison of the properties of oxyhemerythrin with those of deoxyhemerythrin and of the many methemerythrins, in which the Fe atoms have been converted to the Fe(III) oxidation state at the outset. In addition, the properties of appropriate small molecule model iron complexes have been examined.

The absorption spectra of deoxy-, oxy-, and methemerythrin are illustrated in Fig. 7. Methemerythrin, with iron in the Fe(III) oxidation state, forms complexes with each of many small anions (*33*) including N_3^-, NCS^-, NCO^-, Br^-, Cl^-, CN^-, F^-, and OH^-. For two of these, azide (*33*) and thiocyanate (*34*), the stoichiometry of iron to bound ligand, L, has been determined and again found to be 2Fe per ligand. The similarity in spectra of oxyhemerythrin and the methemerythrins suggests (*31, 33*) that the oxidation state in oxyhemerythrin should also be classified as Fe(III). A more detailed analysis of the absorption bands, including a comparison of their wavelengths and intensities with model iron chelates, has also been made (*35*). It is remarkable how similar are the spectra of model oxo-bridged complexes, $L_nFe(III)\text{-}O\text{-}Fe(III)L_n$, to those of methemerythrins and oxyhemerythrin. Thus optical spectra provide strong evidence that the two Fe atoms in hemerythrin are close together, and also that they are linked by an oxo-bridge (Fig. 6), as had been suggested earlier (*33*). Similar conclusions can be reached from an examination of circular dichroic spectra (*35*).

Because the iron atoms are imbedded in a matrix of diamagnetic protein, it is very difficult to measure their magnetic susceptibility in hemerythrin. However, changes in susceptibility can be more readily obtained (Fig. 8). No appreciable changes appear when oxyhemerythrin is converted into the metazide or metfluoride form, or when metaquohemerythrin is changed to the azide, cyanide, or thiocyanate complex. On the other hand, the magnetic susceptibility increases when deoxyhemerythrin is prepared from either oxyhemerythrin or metaquohemerythrin (Fig. 8).

The magnetic susceptibility data show that oxyhemerythrin and the derivatives of methemerythrin exhibit a lower effective magnetic moment than does deoxyhemerythrin, which contains Fe(II) (*31*). The low effective magnetic moment in the Fe(III) compounds could in principle be ascribed either to spin pairing attributable to a strong ligand field or to an antiferromagnetic interaction between the pair of iron atoms in each protein subunit. Mossbauer results support the latter interpretation. Low temperature susceptibilities confirm the conclusions from Mossbauer studies.

Mossbauer spectra have been recorded for hemerythrin (*36, 37*) and for model iron chelates, and pertinent parameters, δ (the isomer shift) and ΔE_Q (the quadrupole splitting), are listed in Table 3. Deoxyhemerythrin shows a simple quadrupole-split pair of lines at all temperatures in the absence of a magnetic field, a pattern indicating that there is but one iron environment. The relatively high value of the isomer shift δ (1.15 mm sec^{-1}), and the large quadrupole splitting ΔE_Q (2.86 mm sec^{-1}) show the compound to be high-spin Fe(II). The various methemerythrin complexes also give simple quadrupole-split spectra indicating that here, as in the deoxy form, each iron site is equivalent. The values of the isomer shift and of the quadrupole splitting in these spectra are very similar to those for the high-spin binuclear Fe(III) model compounds, strongly indicating that methemerythrin complexes contain pairs of coupled high-spin Fe(III) ions. The Mossbauer spectrum of oxyhemerythrin differs from that of the other complexes in that it shows two pairs of quadrupole split doublets of equal intensity. Thus there are two iron environments in oxy-

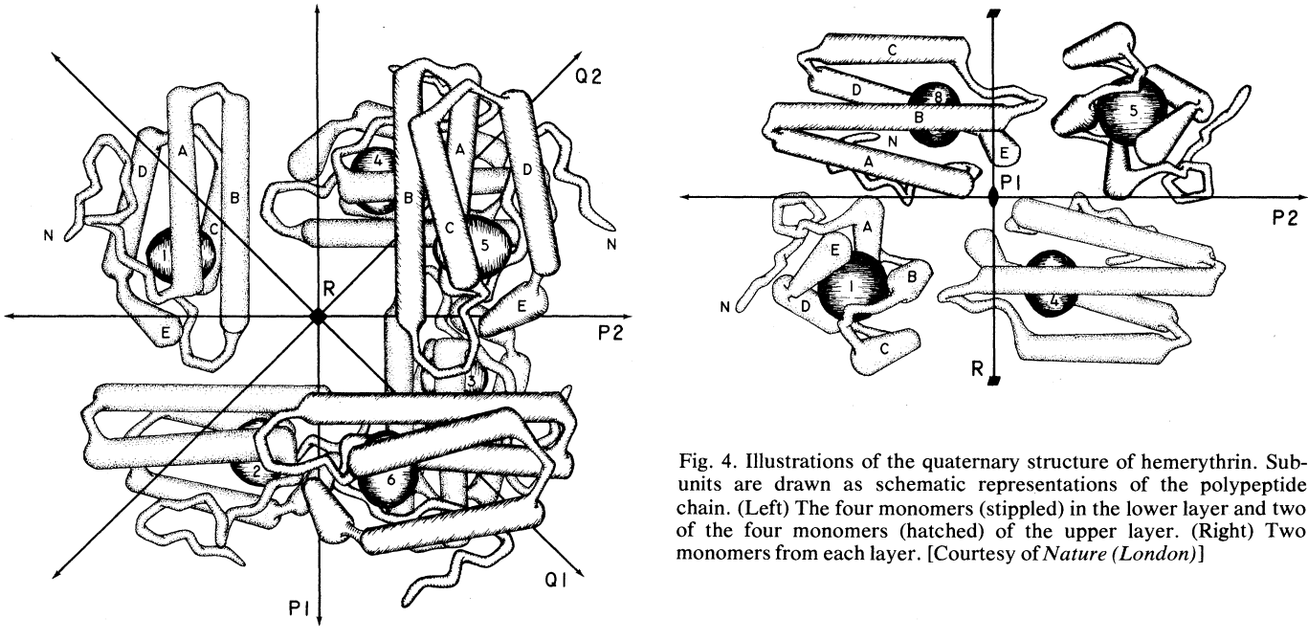

Fig. 4. Illustrations of the quaternary structure of hemerythrin. Subunits are drawn as schematic representations of the polypeptide chain. (Left) The four monomers (stippled) in the lower layer and two of the four monomers (hatched) of the upper layer. (Right) Two monomers from each layer. [Courtesy of *Nature (London)*]

hemerythrin (*37–40*). Nevertheless, the isomer shifts and quadrupole splittings for both oxy doublets are within the range for high-spin, dimeric Fe(III) model complexes.

The effect of a magnetic field at low temperatures is markedly different for (i) a paramagnetic compound as compared to (ii) antiferromagnetically coupled dimers (*38*). The splitting of the spectrum in (ii) can be accounted for by the applied magnetic field. The Mossbauer spectra of oxy-, metaquo-, and met-thiocyanatohemerythrin are unchanged by a 5-kilogauss field at 4.2°K; such behavior is indicative of a diamagnetic state for the iron. The splitting of the Mossbauer spectrum of met-thiocyanatohemerythrin at 4.2°K in a 30-kilogauss magnetic field can be accounted for entirely by the applied magnetic field. The lack of an induced hyperfine field under these conditions is a clear indication of a diamagnetic ground state as would be produced by an antiferromagnetic exchange interaction between the iron atoms (ii). Also at low temperatures the classical susceptibilities of methemerythrin and oxyhemerythrin fall, and in fact near 4.2°K the iron becomes diamagnetic (*39, 40*). The magnitudes of the antiferromagnetic exchange coupling constant, J, have been measured as -77 and -134 cm^{-1} for oxy- and metaquohemerythrin, respectively (*40*). These compare to values of -90 to -131 cm^{-1} for model binuclear oxo-bridged Fe(III) complexes (*41*). Thus the high-spin ($s = 5/2$) Fe(III) atoms must be antiferromagnetically coupled, probably through an oxo bridge.

Additional evidence on the nature of the iron center is provided by x-ray diffraction results. The positions of the two iron atoms in myohemerythrin have been determined quite precisely from native anomalous scattering data at a resolution of 2.8 Å (*10*). The refined positions show that the Fe-Fe distance is 3.44 ± 0.05 Å. This is compatible with an oxo-bridged structure. If an Fe-O distance of 1.80 Å is assumed, this corresponds to an Fe-O-Fe bridging angle of 145° which is within the range from structures of model oxo-bridged dimeric iron complexes. It is clear from native anomalous scattering at a resolution of 5 Å from *T. dyscritum* hemerythrin that the iron atoms are also close together in that structure (*16*).

Coordination of iron to protein. Since there is no heme or other prosthetic group in hemerythrin, the iron atoms presumably are held at the active site by direct coordination to side chains from amino acid residues. Of the 113 residues shown in Fig. 2 only a limited number are capable of participating in metal coordination. The apolar side chains (such as Phe, Ile, and Val) certainly cannot be ligands. Coordination affinities of ligands are usually related to acid-base properties, that is, to their tendency to bind a proton. In general, groups with very high or very low pK values do not form bonds with metal cations. Since the hydroxyl groups of threonine and serine, the guanido group of arginine, the indole nitrogen of tryptophan, and the amide groups of asparagine and glutamine all have pK values in the extreme range, they are unlikely to be involved in iron binding. On the other hand the free amino groups of lysine and the NH_2-terminal glycine are potential ligands. Methionine, cysteine, tyrosine, and histidine are all known to coordinate with iron, in cytochrome c, ferredoxin, transferrin, and hemoglobin, respectively. Although the carboxylate groups of aspartic and glutamic acid are only weakly basic, they are also capable of providing ligands to iron. From these considerations, it can be concluded that the following 43 of the 113 amino acids per subunit in *P. gouldii* hemerythrin are potential ligands to the iron atoms: 11 Lys, 1 Gly, 1 Cys, 1 Met, 7 His, 5 Tyr, 11 Asp, 6 Glu, and 1 Ile.

Group-specific reagents have been used extensively to probe the tertiary structure of a number of proteins. Amino acids that react with these reagents under nondenaturing conditions are usually considered "free," that is, accessible to solvent; those that do not react are assumed to be submerged within the protein matrix. In the case of hemerythrin, nucleophilic groups bound to the irons should be blocked from reaction with

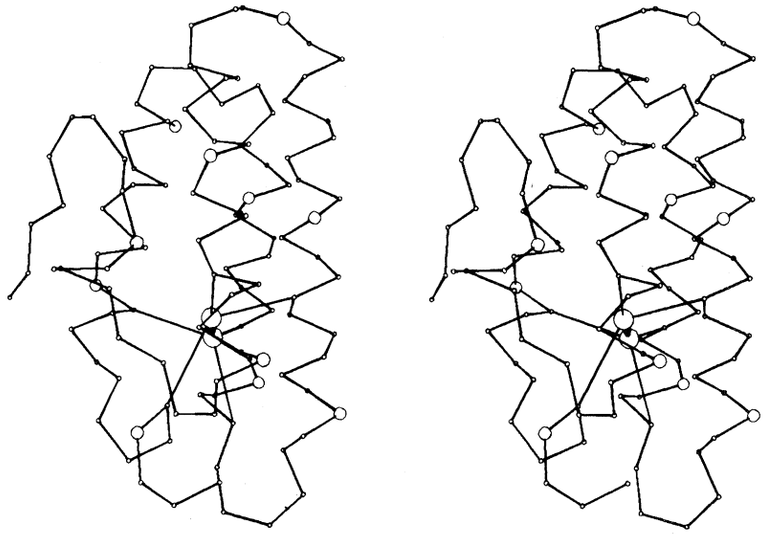

Fig. 5. Stereoscopic drawings of α-carbon backbone models showing active-site iron connections. [Courtesy of *Biochemical Biophysical Research Communications*]

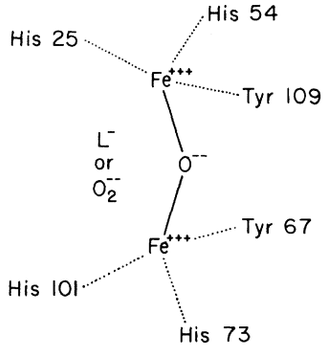

Fig. 6 (left). Details of probable structure at the active site of hemerythrin. Sequence numbering follows Fig. 2. Fig. 7 (right). Visible absorption spectra of hemerythrins. That shown for methemerythrin is with ligands such as Cl^-, OH^-, or OCN^-. Other anion ligands, such as N_3^- and SCN^-, have much stronger absorptions in the range of 500 nm.

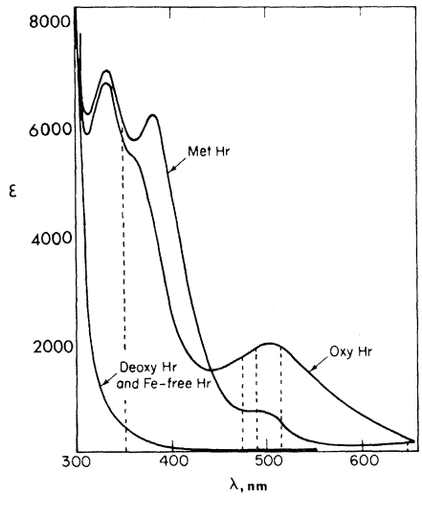

typical electrophiles. However, groups that can undergo ring substitution at positions not directly involved in iron coordination, such as histidine and tyrosine, may participate in chemical reactions.

Modification of hemerythrin by a number of group-specific reagents has yielded some information about its active site. The single Cys of *P. gouldii* hemerythrin can be blocked with typical SH reagents without any accompanying effect on the visible spectrum of the protein (*12*). Such behavior indicates that the SH of Cys-50 (Fig. 2) does not provide an iron ligand. In addition, more recent sequence data show that an SH at position 50 is not essential since it has been replaced by an apolar side chain (Val) in myohemerythrin of *T. pyroides*. Also, the hemerythrin of *Phascolosoma agassizii* contains no Cys residue at all, and yet holds iron in the usual active form. Clearly the SH group is not a ligand to the iron.

Chemical evidence also rules out Lys, Asp, Glu, and Met residues as coordinating groups. All 11 lysines and the NH_2-terminal glycine in *P. gouldii* hemerythrin can be blocked, either by succinylation (*42*), amidination (*42, 43*), or maleylation (*42*) without appreciable changes in the spectral properties of the iron site. Thus, primary amino groups cannot be iron ligands. All carboxyl groups in *P. gouldii* chloromethemerythrin can be modified with glycine methyl ester by use of a water-soluble carbodiimide coupling reagent, yet the modified protein retains the spectral properties of native hemerythrin (*44*). This result rules out Asp, Glu, and the COOH-terminal carboxyl as ligands to the iron site. Experiments in which the single methionine at residue 62 have been alkylated with iodoacetamide tend to rule this group out as an iron ligand as well (*42*). At *p*H 5.5 where alkylation of histidine is minimized, 0.76 residue of methionine can be alkylated without loss of iron, or of the characteristic color of the protein, although the alkylated protein is insoluble at this *p*H. At *p*H 8.0, where modified protein remains soluble, as much as 0.48 of the methionine residue can be alkylated before significant change in the spectral properties of the iron begin. The changes occurring with higher alkylation presumably reflect reaction with His residues.

On the basis of examples such as hemoglobin and cytochrome c, it seemed quite probable that His residues would be among the iron ligands in hemerythrin. An early chemical modification experiment, which appeared to confirm this expectation, revealed that four monosubstituted and three disubstituted histidines were produced upon reaction of *P. gouldii* hemerythrin with diazonium-1*H*-tetrazole (*45*). However, the conclusion that four histidines are iron-linked was not convincing. The chemical basis of the experiment was equivocal, for example, the presumption that substitution occurs at imidazole nitrogens, not carbons, and the idea that monosubstituted imidazole would be the sole product in iron-linked histidines whereas disubstituted imidazole would be the sole product in non-iron-linked residues. More importantly, the integrity of the iron site in modified hemerythrin was uncertain since the pertinent spectral features were totally obscured by the intensely absorbing histidine derivatives. Furthermore, diazonium-1*H*-tetrazole has subsequently been demonstrated to be nonspecific and totally unsuitable for selective protein modification (*46*).

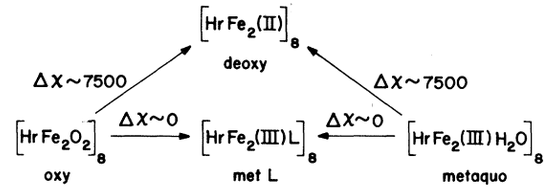

Fig. 8. Changes in magnetic susceptibility accompanying conversion of one form of hemerythrin into another.

However, detailed kinetic studies of the reaction of iodoacetamide with hemerythrin also suggest a role for perhaps four histidines in the active center (*42*). When partially succinylated hemerythrin is allowed to react at *p*H 8 and 30°C with 0.4*M* iodoacetamide, absorption spectra due to the iron chromophore, the iron content, and the fraction of α-helical conformation remain essentially unchanged for 10 to 12 hours. Beyond this time each of these parameters decreases sharply, and after 30 hours of reaction, little further change in these properties occurs; evidently the iron site and native conformation of the protein have been essentially destroyed. During the initial lag period only, more than 1 residue (1.2 residues) of histidine reacts, and less than 1 residue (0.9 residue) when the variant hemerythrin B, which lacks His-82, is modified. The 0.9 residue in hemerythrin B includes partial modification of residue 34 and either residue 73 or 77, these latter two histidines having been recovered in a single peptide. The 1.2 residues modified in the variant hemerythrin A containing residue 82 presum-

Table 3. Comparison of Mössbauer properties of hemerythrin complexes with those of model systems.

Complex	Ligand	Mössbauer parameters*	
		Isomer shift δ (mm/sec)	Quadrupole splitting ΔE_Q (mm/sec)
Deoxyhemerythrin	H_2O	1.15	2.86
Oxyhemerythrin	O_2	0.46 0.47	1.87 0.94
Methemerythrin	NCS^-	0.55	1.92
	Cl^-	0.50	2.04
	F^-	0.55	1.93
	N_3^-	0.50	1.91
	H_2O	0.46	1.57
$[Fe_3O(Ac)_6(H_2O)_3]^{2-}$†		0.43	0.43
$[(Fe(H_2O)B)_2O]^{4+}$		0.54	0.85
$[(FeEDTA)_2O]^{4-}$		0.46	1.44
$[(Fe(-)PDTA)_2O]^{4-}$		0.44	1.74
$[(FeHEDTA)_2O]^{2-}$		0.46	1.68
$[(Fe\ phen_2)_2O]^{4+}$		0.49	1.68
$[(Fe\ bipy_2)_2O]^{4+}$		0.48	1.51
$[(Fe\ terpy)_2O]^{4+}$		0.59	2.35
[(Fe salen)$_2$O]		0.46	0.78
[(Fe (salen)Cl)$_2$]		0.51	1.40

*Mössbauer parameters shown were measured at 77°K, relative to iron foil. Taken from (*38*). Abbreviations are as follows: Ac, acetate; EDTA, ethylenediaminetetraacetate; PDTA, propylenediaminetetraacetate; HEDTA, *N*-hydroxyethylethylenediaminetriacetate; phen, phenanthroline; bipy, bipyridyl; terpy, terpyridyl; salen, *N*, *N'*-bissalicylideneethylenediamine, B, 2,13-dimethyl-3,6,9,12,18-pentaazabicyclo[12.3.1]octadeca-1(18),2,12,14,16-pentaene.

ably includes some modification of this residue during the lag period. These results suggest that histidines -34, -73 or -77, and -82 are not iron ligands. Further alkylation, for a total of 30 hours, results in partial modification of all histidines in the molecule; these observations imply that the remaining four residues, 25, 54, 73 or 77, and 101 (Fig. 2) are iron coordinating groups.

His-34 and His-82 can also be eliminated as ligands from phylogenetic comparisons. Cys-34 and Glu-82 are replacements in myohemerythrin (*18*), and His-82 is also replaced in *P. gouldii* hemerythrin B and *T. pyroides* coelomic hemerythrin (*19, 20*).

Tyrosine residues are also candidates for iron coordination (*47*). Modification with tetranitromethane yields nitrated hemerythrins in which one to two tyrosines are modified, identified as residues 18 and 70 (*48*), with full retention of the iron content, and having the circular dichroic spectrum of the iron site and the normal pK_a of nitrotyrosine. It has also been reported (*49*) that three tyrosines are nitrated in native hemerythrin with minimal iron loss, but in that study the integrity of the iron site was not assessed spectrally. In fact, the reported frictional ratio, diffusion coefficient, and gel filtration behavior of this nitrated protein are consistent only with an extensively denatured molecule. Three tyrosines can be acetylated with *N*-acetylimidazole in hemerythrin in which the lysines have been amidinated, without loss of the spectral character of the active center (*43*). The residues acetylated were not identified but the finding is consistent with the idea that three of the five tyrosines in hemerythrin are not bound to iron. In summary, Tyr-18 and Tyr-70 are clearly excluded from the iron site by chemical modification studies, whereas one or two of the residues 8, 67, and 109 (Fig. 2) are implicated as iron ligands.

Thus of the 44 potential ligands listed at the outset, only 8 are possibilities: His-25, -54, -73, -77, -101, and Tyr-8, -67, and -109. These results have facilitated an interpretation of the low-resolution electron density map of myohemerythrin to give a probable specification of ligand residues and at least a partial description of the geometry of iron coordination (*10*).

In the 5.5-Å map of metazide myohemerythrin, an especially dense spheroidal mass marks the active site region. Six density connections are made from the protein chain to this iron mass. Four of these, one from each major helix, are about in a plane normal to the pseudodiad axis. The other two are from one end of the molecule, one from the E stub and one from the BC corner. Three connections are directed toward one of the iron positions located from native anomalous scattering data, and the other three connections go toward the other iron position. An atomic model recently built to fit this map (*30*) indicates that these connections correspond to His-25, His-54, and Tyr-114 (homologous with Tyr-109 in *P. gouldii* hemerythrin) being attached to the one iron atom and His-73, His-106 (homologous with His-101), and Tyr-67 being attached to the other. The geometry of this configuration is shown in Fig. 5. An alternative, although less likely, arrangement would have His-73 and His-77 in the places of Tyr-67 and His-73, respectively. Density connections are also seen between the iron masses and protein chains in *T. dyscritum* hemerythrin (*16*). These correspond to some but not all of the myohemerythrin assignments.

State of bound oxygen. With the mode of linkage of the metal to the carrier protein reasonably delineated and the electronic state of the iron atoms solidly established, it behooves us to examine the electronic nature of the bound dioxygen, the transport of which is the raison d'être of hemerythrin.

In deoxyhemerythrin, the oxidation state of iron was unequivocally established by chemical means some time ago (*31*) as Fe(II). Spectroscopic and magnetic techniques have now shown that the oxidation state in oxyhemerythrin should be described as Fe(III), with the iron atoms antiferromagnetically coupled. The uptake of dioxygen can thus be described by the following transition:

$$\underset{\text{Fe(II)}}{\underline{|}}\ \underset{\text{Fe(II)}}{\underline{|}}\ + O_2 \longrightarrow \underset{\text{Fe(III)}}{\underline{|}}\ \underset{O_2^{2-}}{\underline{\quad}}\ \underset{\text{Fe(III)}}{\underline{|}}$$

The oxidation state assigned to the oxygen, O_2^{2-}, emerges by implication; the two electrons given up by the 2 Fe(II) of deoxyhemerythrin, to produce 2 Fe(III) in oxyhemerythrin, are assumed to reside on the oxygen. It would clearly be desirable, nevertheless, to have more direct evidence on the electronic state of the oxygen.

Access to such evidence has been given recently by development of techniques, based on resonance Raman spectroscopy, for establishing vibration frequencies of solutes in dilute aqueous solution. A resonance condition may be achieved by illumination of the sample with light of a frequency that lies within an electronic absorption band. Under these circumstances Raman scattering is intensified in vibrational modes associated with the chromophore, other modes being essentially unaffected. As a result, the resonance Raman bands often manifest themselves to the exclusion of all others.

Since the active site of oxyhemerythrin has a strong oxygen-iron charge-transfer band (Fig. 7) centered at 500 nm, resonance Raman spectroscopy becomes attractive as a probe of the electronic state of the atoms, particularly the liganded O_2, at this site.

Excitation of oxyhemerythrin with blue or green lines of an Ar^+ laser generates two Raman bands of moderate intensity (*50*) at 844 and 500 cm^{-1} (Fig. 9). These peaks are not observed with excitation outside of the absorption envelope (Fig. 7), nor are they present in the Raman spectra of deoxyhemerythrin or methemerythrins. Thus it is evident that the chromophoric active site is involved in the expression of these vibrational transitions.

In a test of the presumption that bound oxygen is involved in these resonance-enhanced vibrational modes, oxyhemerythrin labeled with oxygen-18 gas was prepared. The spectrum showed shifted bands, the peak at 844 cm^{-1} going to 798 cm^{-1} and a portion of the peak at 500 cm^{-1} going to 478 cm^{-1}. These isotopic frequency shifts confirm the assignment of these bands to active-site modes, specifically those involving O_2 vibrations.

The frequency ν of the oxygen-oxygen symmetric stretch can be compared to that of diatomic oxygen in other molecular species. Vibrational and structural parameters of model compounds have been assembled (*50*). From these data for small molecules, it is evident that ν_{O-O} stretching frequency reflects the oxidation state of diatomic oxygen. Thus O-O is 1555 cm^{-1} for gaseous O_2, near 1115 cm^{-1} for the superoxide state O_2^-, and in the range of 800 cm^{-1} for O_2^{2-}. The observed frequency in oxyhemerythrin, 844 cm^{-1}, establishes that the bound oxygen is in a peroxide-type electronic state. Thus the Raman spectra provide a direct confirmation of the description of the oxygenation reaction as involving the transfer of $2e^-$ from the two Fe(II) atoms to O_2 to produce a bound peroxide. Figure 6 depicts the O_2^{2-} in this state in the active site.

Environment of the Active Site

The active center of hemerythrin (Fig. 6) might be expected to be in a nonpolar environment on the basis of the relatively large formation constants of heme-

rythrin-anion ligand complexes (*51*). Also close to the active center must be one or two sites for binding of anions such as ClO_4^-, NO_3^-, HCO_3^-, $H_2PO_4^-$ (*51*), and Cl^- (*52*) since binding of such anions decreases the rate of formation and stability of methemerythrin coordination complexes, inhibits reactivity of Cys-50, prevents modification of one or two lysine residues, and increases the oxygen affinity of deoxyhemerythrin (*53*). That a lysine residue is close to the iron locus is evident from the observation that its ionization affects binding of ligands to iron (*54*). Complementarily, binding of ligands affects the pK_a value of this lysine. However, its pK_a is unaffected by anions such as ClO_4^-, and it is thus distant from the ClO_4^- class of binding sites. Another ionizable group, probably an aspartic or glutamic acid, affects and is affected by the coordination of iron ligands (*54*). The pK_a of this acidic residue is changed by the binding of ClO_4^-.

Atomic models derived from even the low-resolution crystallographic analysis permit one to make plausible assignments for the amino acid residues in the neighborhood of the active center. Residues in close proximity to one side of the iron center (that toward top in Figs. 3 and 5) are largely hydrophobic. Among these seem to be Trp-10, Leu-28, Phe-29, Phe-55, Trp-97, Leu-98, and Ile-102. More external groups which may guard this site are Cys-50, Thr-51, Gly-76, and His-77. Hydrophobic residues (Leu-21, Phe-29, and Tyr-70, included) appear to protect the other side of the iron dimer as well, but polar groups other than the ligands identified in Fig. 6 may also approach from this side. Most notable among these is Glu- or Gln-58. Apolar Phe-14, Met-62, Phe-108, and Leu-113 may also contribute to the hydrophobic character of the environment enclosing the active site from this side. Nearly all of the above residues are either invariant or highly conserved among the different hemerythrin sequences.

The binding site for ClO_4^-, and related anions, should also be near the iron center if we are to account for the observed effects on the behavior of the active center and on Cys-50. Inspection of the tentative atomic model (Fig. 5) suggests Arg-49 and Lys-53 as a possible anion-binding site which could affect reactivity at both Cys-50 and the iron center. This area, evidently on the surface of monomeric hemerythrin, would be in the interior of the octameric ensemble, faced by an apolar region from the contact interface of a complementary subunit. Such an environment would account for the strong binding of ClO_4^- by the octamer and predict much weaker binding in the monomer. This prediction has not yet been tested.

Functional groups which are conspicuously close to the iron site are His-77, Tyr-18, Trp-102, and—somewhat farther away—Tyr-8 and Met-62, all of which are invariant. Although not linked to iron in oxy- or methemerythrins, one or more of these residues may function in oxygen binding. One model of oxygen binding in hemerythrin (*37*) involves two basic protein groups which are iron-linked in deoxyhemerythrin and protonated in the oxy form. Although Fe(II) would not be expected to coordinate additional tyrosines because of its characteristically low affinity for oxygen ligands, His-77 might act in this way. Another of these residues might act to stabilize the bridging from protein to the hydroperoxo group in oxyhemerythrin in a manner that results in two iron environments in this form of the protein (*37*). A reorientation of aromatic side chains has been observed, in fact, upon conversion of *Sipunculus nudus* deoxyhemerythrin to the oxy form (*55*), perhaps a reflection of the participation of tyrosines in this transformation. Actual identification of all these residues must await more extensive, high-resolution crystallographic analysis.

After the completion of this manuscript, a preprint became available which describes the structure of the iron complex in *T. dyscritum* methemerythrin as deduced from a 2.8-Å resolution electron density map (*56*). The iron dimer appears to be coordinated by eight protein side chains. By structural homology with the *P. gouldii* sequence, these ligand positions are identified as corresponding to His-25, His-54, and Tyr-109 coordinating to one iron atom, His-73, His-77, and His-101 coordinating to the other iron atom, and Gln-58 and Asp-106 bridging both iron atoms.

Conclusion

Our understanding of the three-dimensional structure of hemerythrin and of the electronic state of the active site is approaching in refinement that currently available for hemoglobin. A comparison of these two oxygen carriers reveals aspects of both unity and diversity in the evolutionary development of cellular molecular devices. Both of these oxygen carriers are constituted of amino acids in polypeptide linkage. Furthermore, both show a very high helix content. At the active site, each uses iron. However, the latter resemblance is superficial, for there is marked divergence in the structural disposition and electronic nature of the metal in the two classes of protein. Incorporation of a single iron atom into the porphyrin ring has provided a system which, imbedded in a protein matrix, can be adapted to provide catalysts of oxido-reduction reactions, with or without direct participation of oxygen (cytochromes, peroxidases), and reversible oxygen binding, transport, and release (myoglobin, hemoglobin). Alternatively, corresponding functions can be imparted to a protein containing no heme at all but incorporating instead pairs of precisely placed, antiferromagnetically coupled iron atoms. With suitable structural modifications one obtains oxido-reduction catalysts (ferredoxins) or reversible oxygen carriers (myohemerythrin, hemerythrin).

In both classes of oxygen carrier, heme or nonheme iron-pair, both genetic and environmental factors modulate the functioning of the protein. Substitutions of residues in the primary structure, in consequence of genetic mutation, can lead to marked changes in oxygen affinity or in oligomeric state in hemerythrin or hemoglobin. Both classes of protein are also capable of transmitting impulses from bound solutes originating from the aqueous environment. In the course of

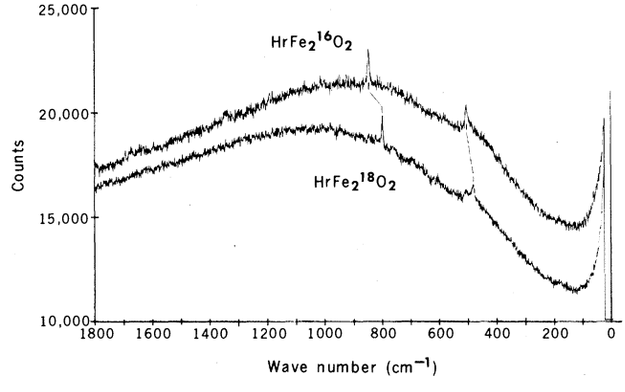

Fig. 9. Resonance Raman spectra of oxyhemerythrin in solution. [Courtesy of *Biochemistry*]

evolution, nature has been able to find more than one efficient molecular mechanism for maintaining a vital organismic function.

References and Notes

1. F. Hoppe-Seyler, *Virchows Arch. Pathol. Anat. Physiol.* **19**, 233 (1864).
2. I. M. Klotz and S. Keresztes-Nagy, *Biochemistry* **2**, 445 (1963).
3. G. Bates, M. Brunori, G. Amiconi, E. Antonini, J. Wyman, *ibid.* **7**, 3016 (1968); R. E. Ferrell and G. B. Kitto, *ibid.* **9**, 3053 (1970); W. A. Hendrickson and G. L. Klippenstein, *J. Mol. Biol.* **87**, 147 (1974).
4. G. L. Klippenstein, D. A. Van Riper, E. A. Oosterom, *J. Biol. Chem.* **247**, 5959 (1972).
5. J. G. Joshi and B. Sullivan, *Comp. Biochem. Physiol. B* **44**, 857 (1973).
6. F. A. Liberatore, M. F. Truby, G. L. Klippenstein, *Arch. Biochem. Biophys.* **160**, 223 (1974).
7. J. S. Loehr, K. N. Meyerhoff, L. C. Sieker, L. H. Jensen, *J. Mol. Biol.* **91**, 521 (1975).
8. I. M. Klotz, D. W. Darnall, N. R. Langerman, in *The Proteins*, H. Neurath and R. Hill, Eds. (Academic Press, New York, ed. 3, 1975), vol. 1, pp. 293–411.
9. D. W. Darnall and I. M. Klotz, *Arch. Biochem. Biophys.* **166**, 651 (1975).
10. W. A. Hendrickson, G. L. Klippenstein, K. B. Ward, *Proc. Natl. Acad. Sci. U.S.A.* **72**, 2160 (1975).
11. K. B. Ward, W. A. Hendrickson, G. L. Klippenstein, *Nature (London)* **257**, 818 (1975).
12. S. Keresztes-Nagy and I. M. Klotz, *Biochemistry* **2**, 923 (1963).
13. I. M. Klotz and S. Keresztes-Nagy, *Nature (London)* **195**, 900 (1962).
14. B. W. Matthews and S. A. Bernhard, *Annu. Rev. Biophys. Bioeng.* **2**, 257 (1973).
15. A. C. T. North and G. J. Stubbs, *J. Mol. Biol.* **88**, 125 (1974).
16. R. E. Stenkamp, L. C. Sieker, L. H. Jensen, J. S. Loehr, *ibid.* **100**, 23 (1976).
17. A. R. Subramanian, J. W. Holleman, I. M. Klotz, *Biochemistry* **7**, 3859 (1968); G. L. Klippenstein, J. W. Holleman, I. M. Klotz, *ibid.*, p. 3868.
18. G. L. Klippenstein, J. L. Cote, S. E. Ludlam, *ibid.* **15**, 1128 (1976).
19. R. E. Ferrell and G. B. Kitto, *ibid.* **10**, 2923 (1971).
20. G. L. Klippenstein, *ibid.* **11**, 372 (1972).
21. F. A. Liberatore, thesis, University of New Hampshire (1974).
22. Abbreviations of the amino acid residues are Ala, alanine; Asp, aspartic acid; Asn, asparagine; Arg, arginine; Cys, cysteine; Glu, glutamic acid; Gln, glutamine; Gly, glycine; His, histidine; Ile, isoleucine; Leu, leucine; Met, methionine; Phe, phenylalanine; Pro, proline; Ser, serine; Thr, threonine; Val, valine; Tyr, tyrosine; and Trp, tryptophan.
23. G. L. Klippenstein, unpublished.
24. D. W. Darnall, K. Garbett, I. M. Klotz, S. Aktipis, S. Keresztes-Nagy, *Arch. Biochem. Biophys.* **133**, 103 (1969).
25. G. Holzwarth and P. Doty, *J. Am. Chem. Soc.* **87**, 218 (1965).
→ P. Y. Chou and G. D. Fasman, *Biochemistry* **13**, 222 (1974).
27. J. B. R. Dunn, thesis, Northwestern University (1974).
28. M. Florkin, *Arch. Int. Physiol.* **36**, 247 (1933); W. E. Love, *Biochim. Biophys. Acta* **23**, 465 (1957).
29. I. M. Klotz, T. A. Klotz, H. A. Fiess, *Arch. Biochem. Biophys.* **68**, 284 (1957).
30. W. A. Hendrickson and K. B. Ward, *Biochem. Biophys. Res. Commun.* **66**, 1349 (1975).
31. I. M. Klotz and T. A. Klotz, *Science* **121**, 477 (1955).
32. E. Boeri and A. Ghiretti-Magaldi, *Biochim. Biophys. Acta* **23**, 465 (1957).
33. S. Keresztes-Nagy and I. M. Klotz, *Biochemistry* **4**, 919 (1965).
34. M. H. Klapper and I. M. Klotz, *ibid.* **7**, 223 (1968).
35. K. Garbett, D. W. Darnall, I. M. Klotz, R. J. P. Williams, *Arch. Biochem. Biophys.* **135**, 419 (1969).
36. M. Y. Okamura, I. M. Klotz, C. E. Johnson, M. R. C. Winter, R. J. P. Williams, *Biochemistry* **8**, 1951 (1969); J. L. York and A. J. Bearden, *ibid.* **9**, 4549 (1970).
37. K. Garbett, C. E. Johnson, I. M. Klotz, M. Y. Okamura, R. J. P. Williams, *Arch. Biochem. Biophys.* **142**, 574 (1971).
38. M. Y. Okamura and I. M. Klotz, in *Inorganic Chemistry*, G. L. Eichhorn, Ed. (Elsevier, Amsterdam, 1973), chap. 11.
39. T. H. Moss, C. Moleski, J. L. York, *Biochemistry* **10**, 840 (1971).
40. J. W. Dawson, H. B. Gray, H. E. Hoenig, G. R. Rossman, J. M. Schredder, R. H. Wang, *ibid.* **11**, 461 (1972).
41. K. S. Murray, *Coord. Chem. Rev.* **12**, 1 (1974).
42. J. A. Morrissey, thesis, University of New Hampshire (1971).
43. C. C. Fan and J. L. York, *Biochem. Biophys. Res. Commun.* **47**, 472 (1972).
44. G. L. Klippenstein, *ibid.* **49**, 1474 (1972).
45. C. C. Fan and J. L. York, *ibid.* **36**, 365 (1969).
46. S. F. Andres and M. Z. Atassi, *Biochemistry* **12**, 942 (1973).
47. J. L. York and C. C. Fan, *Fed. Proc. Fed. Am. Soc. Exp. Biol.* **29**, 463 (1970); R. L. Rill and I. M. Klotz, *Arch. Biochem. Biophys.* **136**, 507 (1970).
48. R. M. Rill and I. M. Klotz, *Arch. Biochem. Biophys.* **147**, 226 (1971).
49. J. L. York and C. C. Fan, *Biochemistry* **10**, 1659 (1971).
50. J. B. R. Dunn, D. F. Shriver, I. M. Klotz, *Proc. Natl. Acad. Sci. U.S.A.* **70**, 2582 (1973); *Biochemistry* **14**, 2689 (1975).
51. K. Garbett, D. W. Darnall, I. M. Klotz, *Arch. Biochem. Biophys.* **142**, 455 (1971).
52. A. L. Rao and S. Keresztes-Nagy, *Biochim. Biophys. Acta* **313**, 249 (1973).
53. H. A. DePhillips, *Arch. Biochem. Biophys.* **144**, 122 (1971).
54. K. Garbett, D. W. Darnall, I. M. Klotz, *ibid.* **142**, 471 (1971).
55. F. Bossa, M. Brunori, G. W. Bates, E. Antonini, P. Fasella, *Biochim. Biophys. Acta* **207**, 41 (1970).
56. R. E. Stenkamp, L. C. Sieker, L. H. Jensen, *Proc. Natl. Acad. Sci. U.S.A.* **73**, 349 (1976).

57. Supported in part by NIH grant HL-08299, NSF grant GB-35610, and Naval Research Laboratory.

Educational Uses of the PLATO Computer System

The PLATO system is used for instruction, scientific research, and communications.

Stanley G. Smith and Bruce Arne Sherwood

The PLATO (*1*) computer-based educational system has been specifically designed to provide interactive, self-paced instruction to large numbers of students (*2*). Lesson material is displayed on a screen 22 centimeters square and may consist of text, drawings, graphs, and color photographs. Students interact with the material through a special keyset that closely resembles a typewriter keyboard, and they receive essentially instantaneous reinforcement of correct work and assistance where they are having difficulty. Students can work at their convenience in classrooms such as the one shown in Fig. 1.

The users of PLATO range from grade school students learning reading and math to graduate students in the medical sciences. The system now has 950 terminals located in universities, colleges, community colleges, public schools, military training schools, and commercial organizations (*3*). The users have access to more than 3500 hours of instructional material in more than 100 subject areas (*4*). We will mainly describe one area of PLATO use—that of university science education and research.

Dr. Smith is professor of chemistry at the University of Illinois, Urbana 61801. Dr. Sherwood is associate professor of physics and assistant director of the Computer-Based Eduction Research Laboratory at the University of Illinois, Urbana.

Examples of PLATO Lessons

The character of PLATO lesson material varies greatly since the computer system does not impose a pedagogical structure on the authors of the materials. Some appreciation of the breadth of approaches used may be gained by reviewing brief segments of a few programs in chemistry (*5*) and physics (*6*). The examples below are illustrated with photographs of the student's plasma-panel screen (*7*). Unfortunately, however, these static photographs do not fully convey the dynamic nature of the interactively changing displays seen by the student.

A physics lesson on oscillations contains features common to many expository science lessons. The student is given a table of contents for the lesson so